Supplement of Atmos. Meas. Tech., 18, 3247–3265, 2025
https://doi.org/10.5194/amt-18-3247-2025-supplement

Atmospheric Measurement Techniques
Open Access
EGU

Supplement of

Intercomparison of tropospheric ozone column datasets from combined nadir and limb satellite observations

Carlo Arosio et al.

Correspondence to: Carlo Arosio (carloarosio@iup.physik.uni-bremen.de)

Supplementary Information

This documents presents several plots to support the material displayed in the manuscript.

Figure S1 displays the annual mean climatology for the selected TOR data sets. In the title of each subplot, we report the mean global TrOC values and their standard deviations.

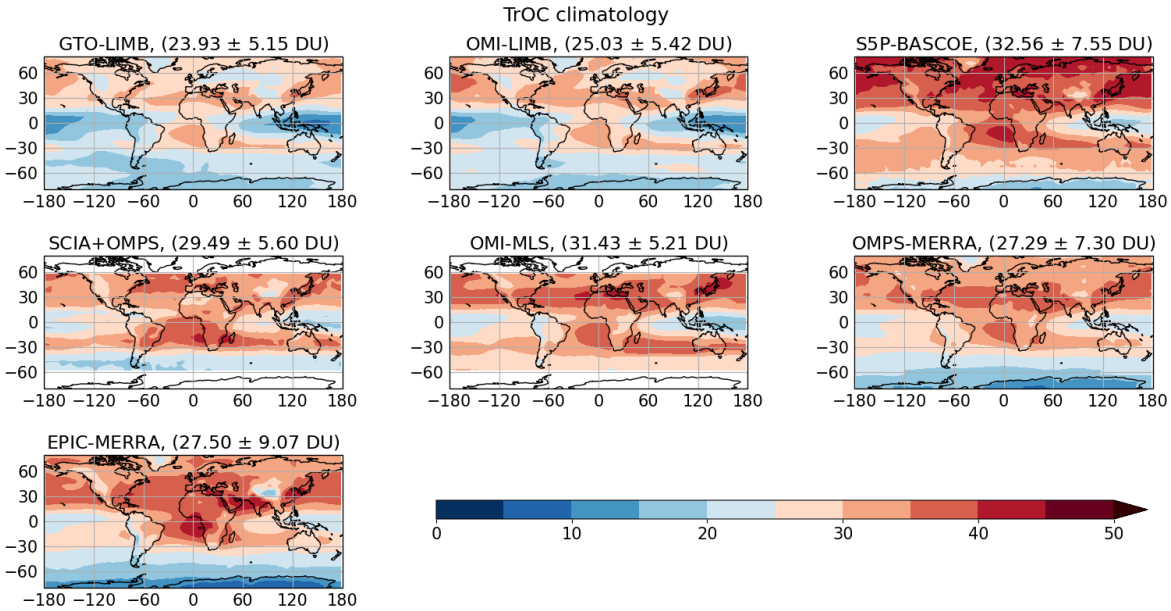

Figure S1: Tropospheric ozone climatology of the seven satellite data sets used for this study. In parenthesis the respective global averages and standard deviations are indicated.

We notice an overall bias present between the maps: global average ozone values are reported in the titles of the subplots and they differ by up to 8-10 DU (from 23.9 DU for GTO-LIMB to 32.5 for S5P-BASCOE, with high TrOC values especially in the northern hemisphere). These biases have several possible reasons: e.g., the TOC and SOC biases between different satellites, the tropopause definition adopted to construct the TOR product, the climatology used to fill stratospheric profile gaps, the criteria used for the subtraction between TOC and SOC. Fig. 1 in the manuscript showcases the biases in terms of zonal means.

Regarding the drop in TrOC occurred after 2020, Fig. S2 shows TrOC anomalies as in Fig.4 of the manuscript, when the seasonal cycle used to obtain anomalies is computed over the 2016-2019 period only, instead that over each respective whole time frame. Figure S3 displays the time series of the data sets at 42.5°N in terms of anomalies, when subtracting the seasonal cycle computed over the respective time period (top panel) or only over 2016-2019 (bottom panel). We can better identify the drop in 2020 and the lower values of the anomalies over the 2020-2022 period, especially if the 2016-2019 seasonal cycle is subtracted. The only data set not showing any drop is S5P-BASCOE.

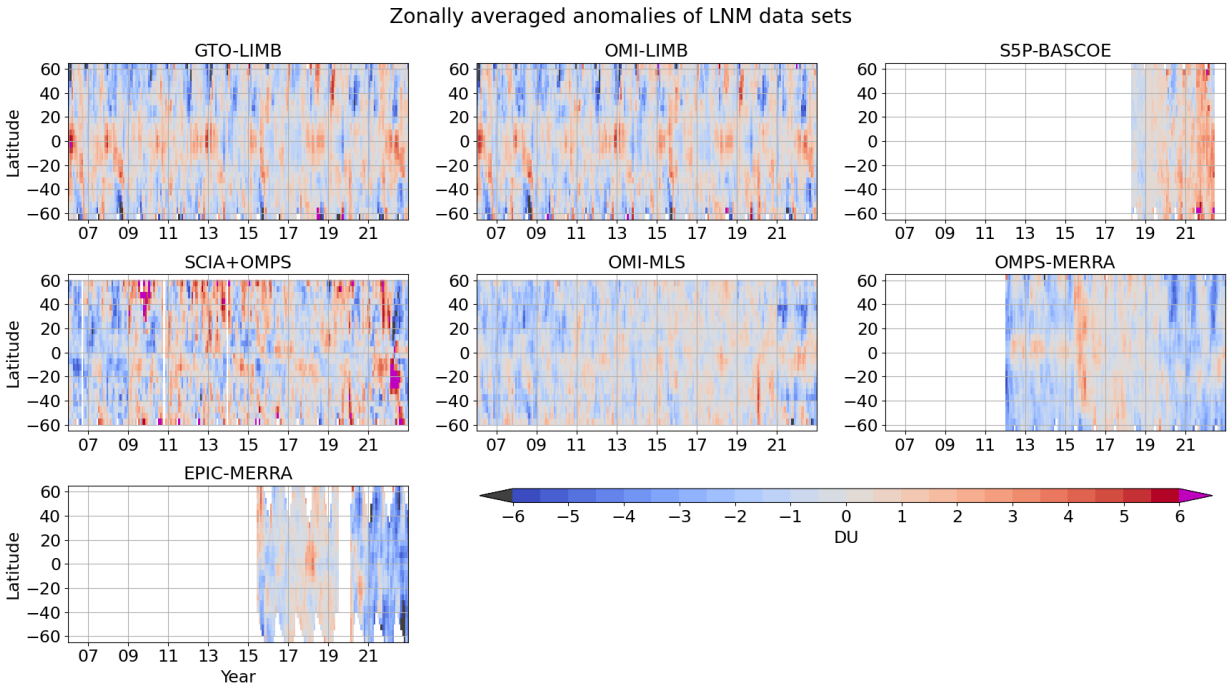

Figure S2: De-seasonalized time series (using the 2016-2019 seasonal cycles) as a function of latitude for the seven data sets.

Figure S4 shows the time series of the TPH absolute anomalies for the selected data sets as a function of latitude, yearly averaged to have a better visualization of the main patterns. Very similar features are found in the data sets, with the largest discrepancy found for OMPS-MERRA (MERRA-2 meteorology), which shows pattern with a smaller amplitude w.r.t. the others. SCIA+OMPS displays large anomalies at mid-latitudes due to a discrepancy between the TPH seasonal cycle extracted from ERA5 for SCIAMACHY and OMPS observations, related to different sampling patterns between SCIAMACHY and OMPS LNM datasets.

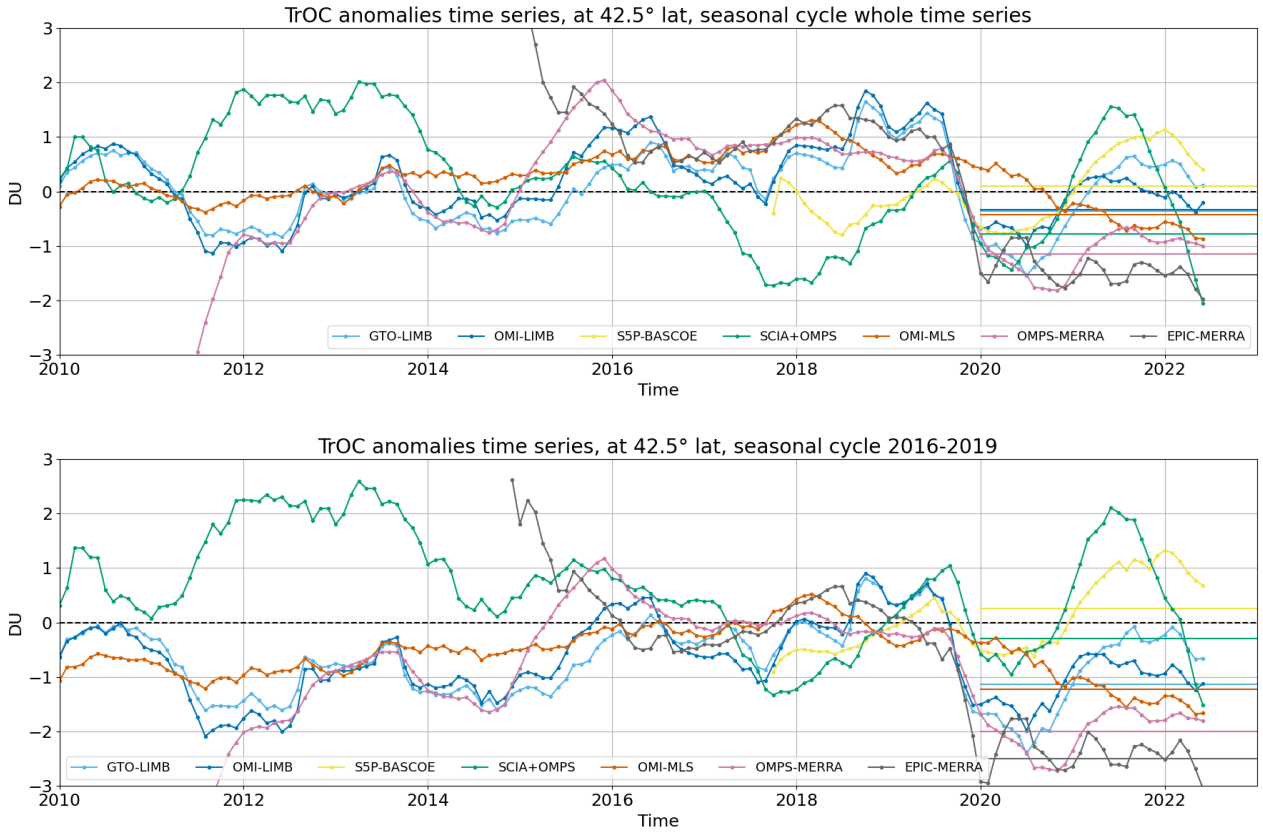

Figure S3: De-seasonalized time series at 42.5°N, using the seasonal cycles computed over the respective time series (top panel) or over 2016-2019 (bottom panel).

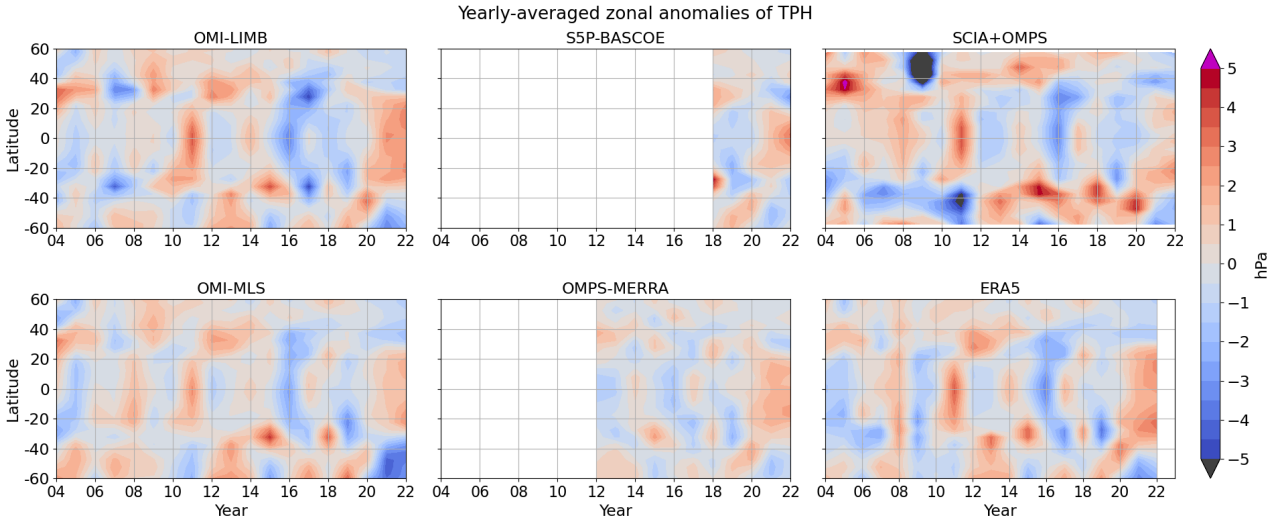

Figure S4: Time series of yearly-averaged zonal absolute anomalies of TPH.

Figure S5 showcases the difference between a TPH correction performed at L2 or at L3. The left panel shows a map of the differences between two SCIAMACHY TrOC data sets obtained using different TPH definitions during the LNM process (the one used

for the SCIA+OMPS product and the TOAR one, i.e. fixed pressure level depending on latitude). The SCIAMACHY TrOC differences are multi-year averages and are compared to ozonesonde sub-columns (in colored dots), which correspond to the ozone content between the two TPH definitions. The right panel shows the results obtained by adjusting the L3 data to take into account this TPH difference, by using a monthly climatology ("IUP 2018"). In this case the correction in TrOC are significantly different to the ozonesonde sub-columns (same as left panel).

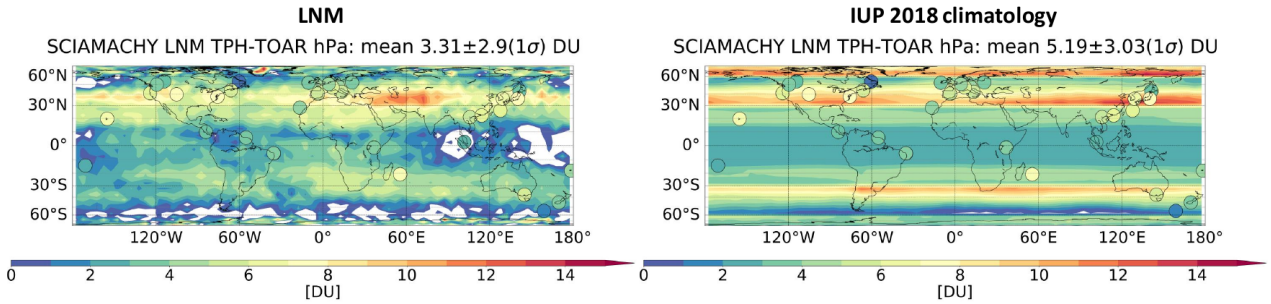

Figure S5: Differences between two SCIAMACHY TrOC data sets obtained using different TPH definitions at the LNM process (the one used for SCIA+OMPS product and the TOAR one). In the left panel the correction is done based on the L2 data, on the right L3 monthly data are corrected for the different TPH using a climatology. The circle show the ozone sub-columns from ozonesonde data between the two TPH definitions.

Table S1 reports the list of ozonosonde stations used for this work, including their locations and data providers. All ozonesonde data used for the study are HEGIFTOM-homogenised.

Table S1: List of the used sonde stations used in this study.

Station	Latitude	Longitude	Data provider
Edmonton	53.55	-114.10	WOUDC
Goose Bay	53.29	-60.39	WOUDC
Legionowo	52.40	20.97	NASA-AMES
De Bilt	52.10	5.18	WOUDC
Valentia	51.94	-10.25	WOUDC
Uccle	50.80	4.35	WOUDC
Kelowna	49.47	-119.38	WOUDC
Hohenpeissenberg	47.80	11.01	WOUDC
Payerne	46.49	6.57	WOUDC
Haute-Provence	43.94	5.71	NASA-AMES
Yarmouth	43.87	-66.11	WOUDC
Trinidad Head	40.80	-124.16	NOAA
Madrid	40.47	-3.58	WOUDC
Boulder	40.13	-105.24	NASA-AMES
Izania	28.31	-16.50	WOUDC
Hanoi	21.20	105.80	SHADOZ
Hilo	19.58	-155.07	SHADOZ
Costarica	9.98	-84.21	SHADOZ
Paramaribo	5.80	-55.21	SHADOZ
Kuala Lumpur	2.73	101.27	SHADOZ
San Cristobal	-0.92	-89.62	SHADOZ
Nairobi	-1.27	36.80	SHADOZ
Natal	-5.42	-35.38	SHADOZ
Watukosek	-7.5	112.6	SHADOZ
Ascension Island	-7.97	-14.40	SHADOZ
Samoa	-14.23	-170.56	SHADOZ
La Reunion	-21.06	55.48	SHADOZ
Irene	-25.9	28.22	SHADOZ

Figure S6 shows a point-to-point correlation map of TrOC values. This was used to define geographical regions where the SC of the several data sets is coherent. In this case the reference location is off-coast of west Africa, identified with a white cross.

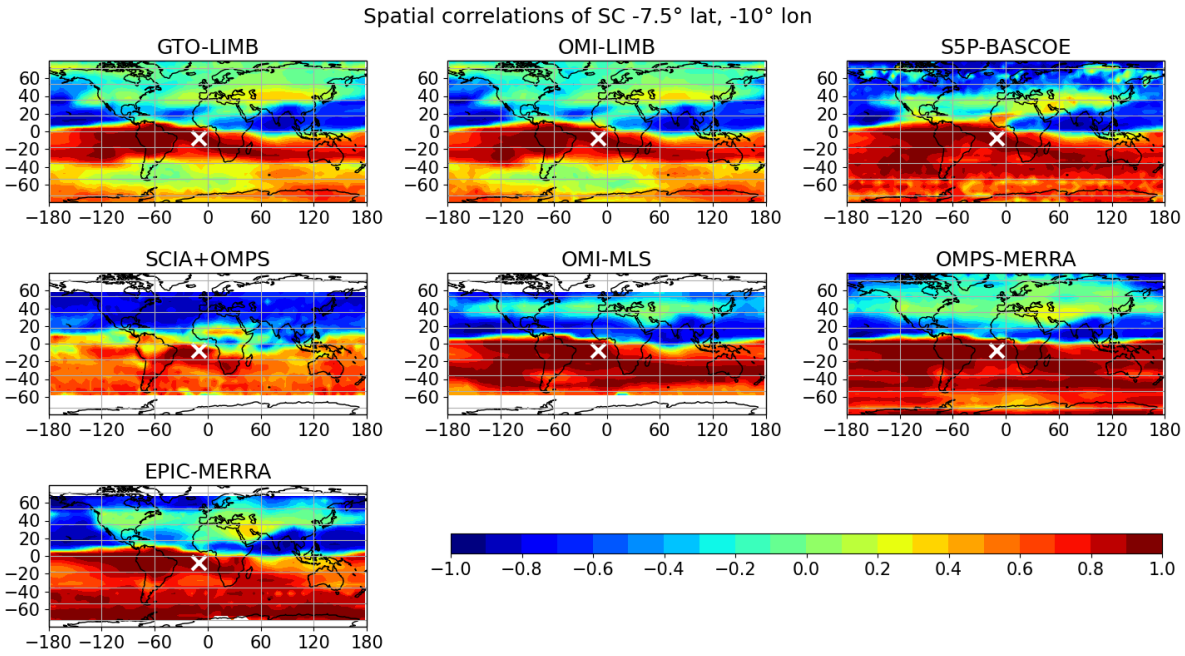

Figure S6: Correlation of the seasonal cycle (SC) of all data sets w.r.t. the location at 7.5°S, 10°W identified with a white cross on the maps.

Figure S7 shows the signature of QBO and ENSO proxies in GTO-LIMB time series, as an example, at two locations where these proxies show high correlations to ozone. We think that the QBO signature is mostly related to the contamination of the stratospheric signal when computing limb-nadir residuals. For HEGIFTOM only in the time series for Nairobi we found a noticeable QBO signature.

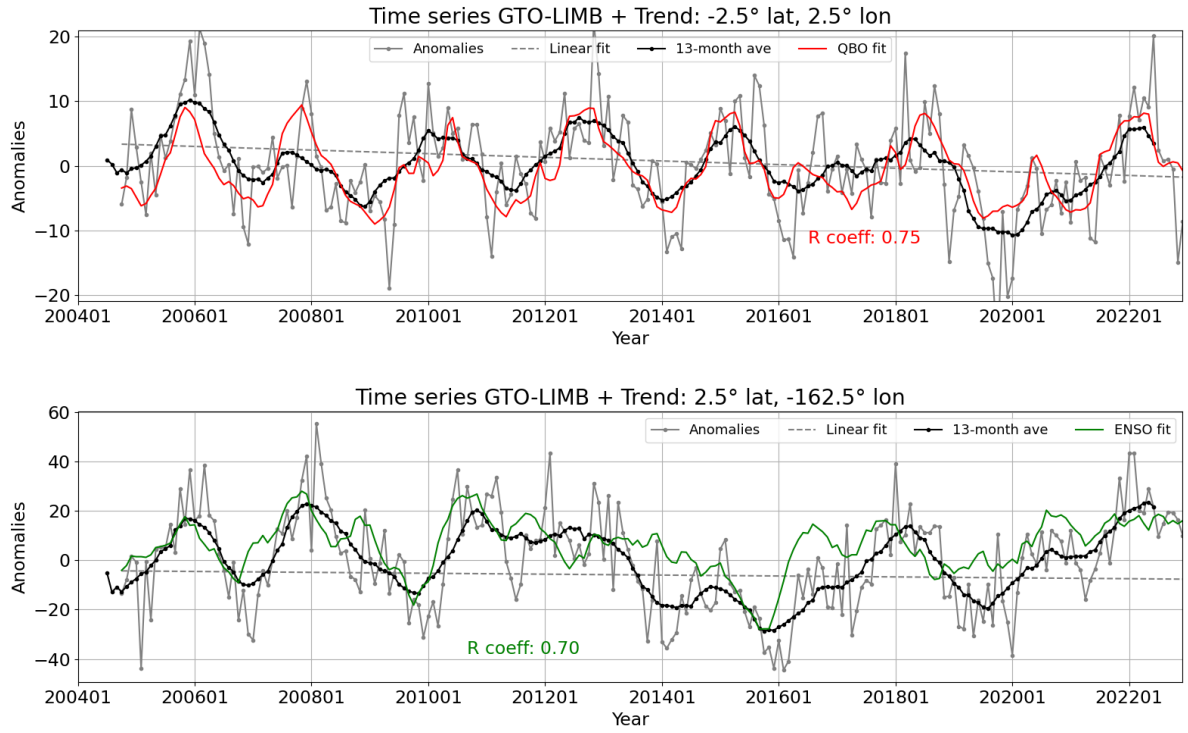

Figure S7: In the first two panels, GTO-LIMB time series at the reported latitude-longitude bin is regressed using QBO and ENSO proxies: the respective fit contributions are over-plotted.

Figure S8 shows the time series and respective trends for three data sets over Europe and the Mediterranean. In the top panel trends from the monthly time series are computed, showing slightly negative mostly non-significant trends. In the second panel summer-time trends are computed, with negative significant trends evident in by the OMI-LIMB data set. Over the Mediterranean, negative and significant summer-time trends are shown by all data sets.

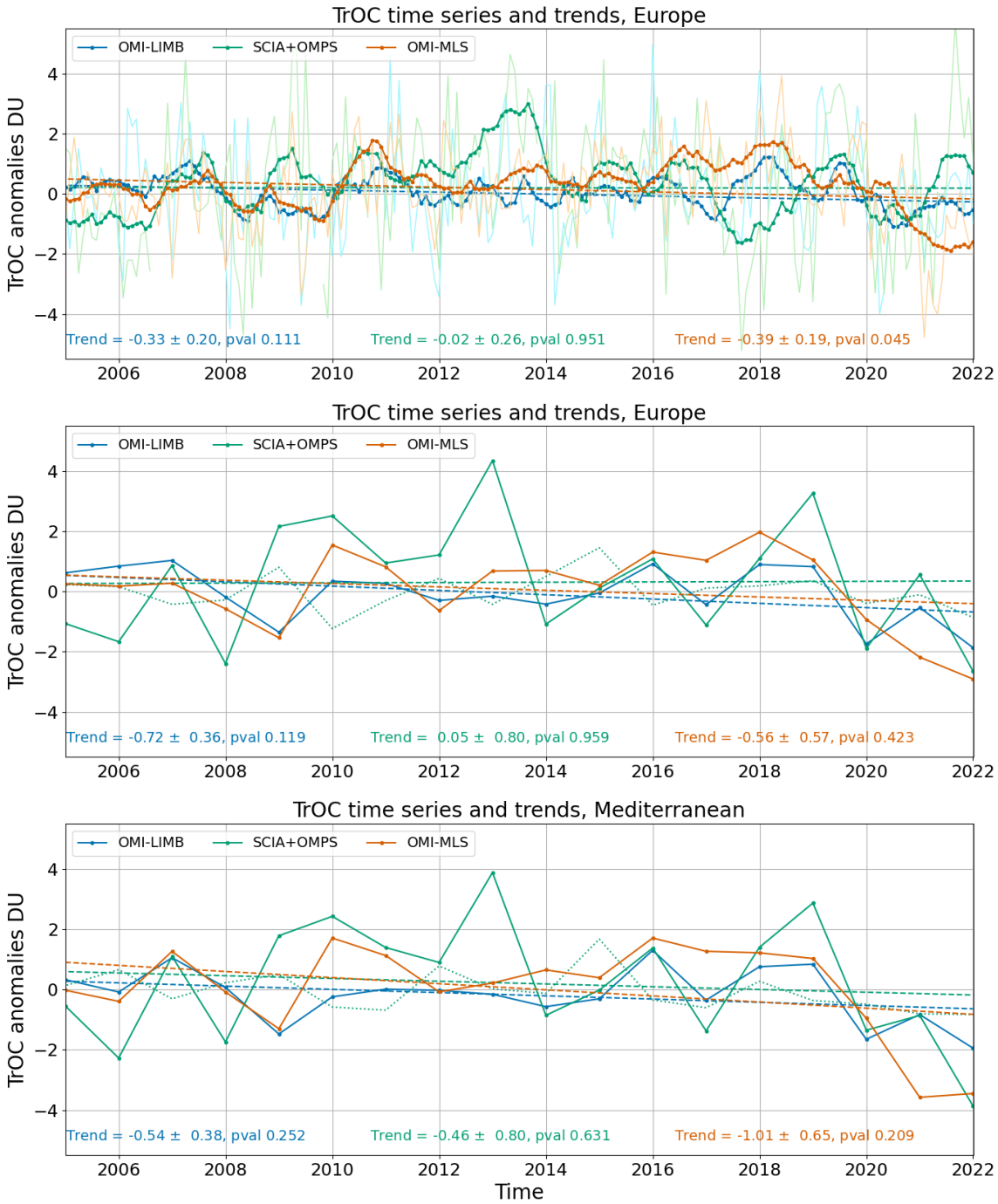

Figure S8: Top panel: time series and trends of the monthly time series averaged over Europe. Middle and bottom panels: summer-time time series and trends over Europe and the Mediterranean, respectively.

Figure S9 shows an example of OMI AK with their crude approximation in red, which has been parametrized as in Eq. A1.

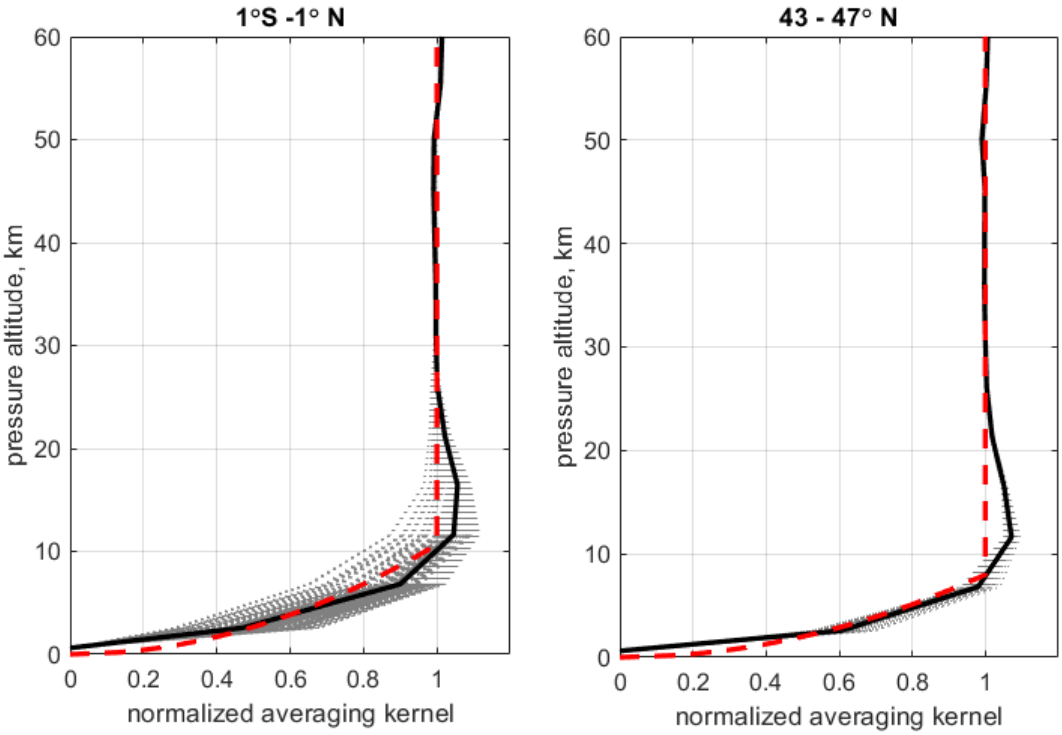

Figure S9: OMI individual averaging kernels normalized to 1 above 25 km (grey lines) for clear-sky conditions on 1 July 2008, the mean averaging kernels (black lines) and their crude approximation (red dashed lines). Left: latitudes [1°S, 1°N], Right: latitudes [43°N, 47°N].